Simulation of Cake Formation for Nano-Fibrous Filter Media Using Image Processing

Maryam Salehi Esfandarani, Morteza Vadood and Majid Safar Johari

Abstract—**Electrospun nano-fibrous webs have great potential in application in high efficiency air cleaning systems. In filtration process, the formation of cake on the filter media causes pressure drop that increase the filtration efficiency. Pressure drop of fibrous media is a function of cake characteristics such as porosity and air permeability. In this paper, the cake formation on nano-fibrous filter media is simulated using an image processing technique. The effects of particles' characteristics, such as shape, size and configuration on cake porosity are investigated using the newly developed algorithm. Results of simulation show that the larger particles in air stream cause higher cake porosity.**

Key words: Nano-fibrous filter media, cake, pressure drop, image processing

I. INTRODUCTION

Filtration is the most important method for removing suspended particles from the air stream. Fibers in nanometric scale provide small pore size and a large surface collection area for nano-fibrous filter media [1]. Electrospun nanofibrous media, with fibers of diameters of 10–100 times smaller than melt-blown and spun-bond filaments, have showed to significantly improve the efficiency of air filtration in particles separation [2]. Low basis weight, high permeability, small pore size, high specific surface area (ranging from 1 to 35m^2/g depending on the diameter of fibers), good interconnectivity of pores and potential to incorporate active chemistry or functionality on a nanoscale are some significant characteristics that cause nanofibrous filter media to be distinct from other fibrous [3].

Cake forms on the filter media when a particle containing gas stream is forced to pass through the filter media [4]. Resistance against the flow of filter media and the cake causes some increments in the pressure drop in the filtration process [5]. Recent studies showed that cake characteristics such as its porosity and permeability are affecting the particle removal efficiency and pressure drop in the filtration process [6-8]. Cake formation process was simulated in 3-D nano-fibrous filter media at reduced pressure drop for different monodisperse and polydisperse aerosols [9]. Lin *et al.* discussed on the experimental results of 3-D cake pore structure that were obtained from X-Ray microtomographic and compared with the Monte Carlo simulation's results [10]. Joubert *et al.* developed a model of variation in the pressure drop across a HEPA filter [11]. The model was based on the filtration process in the presence of humidity and the pressure drop was considered as the sum of pressure drop across the clean filter and across the cake. A statistical model was developed in order to predict the cake thickness, cake porosity, pressure drop and filtration efficiency across the clogged filter media. Results indicated that increasing the cake thickness causes average cake porosity to decrease, also pressure drop increases with decreasing particle size [12].

Image processing algorithms were recognized as the powerful methods to characterize the nanofibrous structures [13]. Ghasemi and her colleagues used the image processing to measure the porosity of nanofibrous scaffold in the various layers by counting the dark and white pixels [14]. Semnani *et al.* predicted the cell infiltration in the nanofibrous scaffold by applying a cell matrix as mask through the scaffold matrix [15]. In this paper, a new image processing algorithm is presented to simulate the cake formation on the nano-fibrous filter media. Additionally, cake formation is compared for particles with various shapes and sizes.

M. Salehi Esfandarani, M. Vadood and M. Safar Johari are with the Department of Textile Engineering of Amirkabir University of Technology, Tehran, Iran. Correspondence should be addressed to M. Vaddod (e-mail: mortezavadood@aut.ac.ir).

II. EXPERIMENTAL

Polyacrylonitrile (PAN) with the weight-average molecular weight (Mw) of 100,000 g/mol was kindly supplied by Polyacryl Iran Company. N, N-dimethylformamide (DMF) and Silica (SiO_2) nanoparticles were provided by Merck and Nabond, respectively. A homogenous dispersion of silica nanoparticles in the PAN solution in DMF was electrospun. The morphology of nano-fibrous filter media was observed by a field emission scanning electron microscope (HIT S-4160) at 15 kV0. The FE-SEM scan of electrospun nano-fibrous web is shown in Figure 1 with the magnification of X15000. Higher degree of magnification led to incomplete scan of surface of nanofibrous. Oppositely, with the lower degree of magnification, the pore areas were not sufficiently distinguishable from the fibers. Mean fiber diameter and its coefficient of variance were 205 nm and 17%, respectively.

III. IMAGE PROCESSING APPROACH

A. *Determination of thresholds value*

Considering the gray scale of FE-SEM image in Figure 1 shows that the nano-fibers' pixels in the upper layer

benefit from higher intensity in comparison to the pixels that locate in the down layers. So, determination of threshold level would be a critical parameter in converting the gray scale images to the binary.

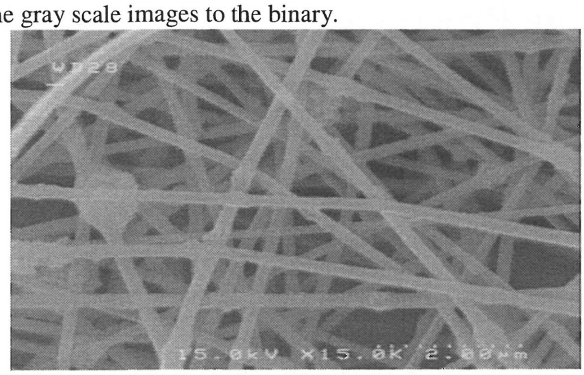

Fig. 1. FE-SEM scan of nano-fibrous web.

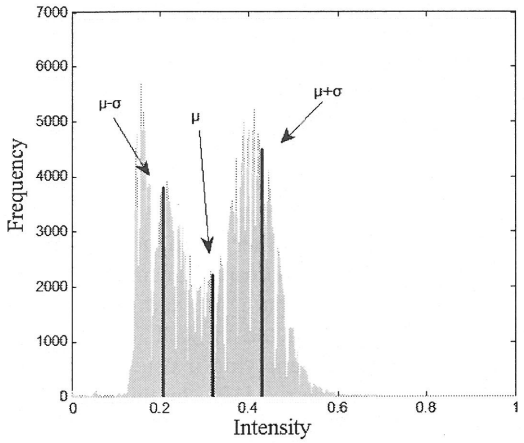

Fig. 2. The histogram of pixels intensity values in gray scale of FE-SEM scan of nanofibers.

By selecting of lower threshold value more layers in the SEM image become apparent in the binary image. Considering the shape of intensity histogram of SEM image shows that there are two peaks and one cavity in the intensity histogram of nano-fibrous image (Figure 2). The peaks and cavity are related to μ and $\mu \pm \sigma$ (μ and σ are mean and standard deviation of intensity of pixels). It was found that by using μ and $\mu \pm \sigma$ as threshold values, the SEM image can be divided into three different layers and cake formation could be simulated on these layers in the nano-fibrous web. The porosity of the nano-fibrous web was determined by counting dark (N_D) and light pixels (N_L) according to Eq. (1).

$$\text{Porosity} = \frac{N_L}{N_L + N_D} \tag{1}$$

The selected thresholds and the corresponding resulted porosity are shown in Table I, and the binary images resulting from the desired thresholds are shown in Figure 3. The web porosities show that by decreasing the threshold values, deeper layers become more apparent and consequently web porosity based on the Equation 1 decreases.

IV. Infiltration of Cells through the Fibrous Filter Media

Since particles' shapes could affect the filtration efficiency [16], the cake formation in this research was simulated for particles with different shapes (Figure 4). The angle between the horizontal axis and the major diameter for the ellipse cells were considered 0°, 25°, 45°, 70° and 90°. The diamond cell was considered as a square cell which was rotated 90°. These shapes just simplified the real shape of particles that usually have irregular shapes and their equivalent diameters would be considered in calculations. Obviously, the most important shapes would be circular and square that were used in this research. The deviation from circular shape was also considered in this work by using an ellipse shape. Clearly, when the particles approached to the filter surface they may find different configurations and places on the filter in different angles. So, such shapes just simplified the parameters of shapes and configurations.

TABLE I
THE THRESHOLDS OF IMAGES

Threshold	Value	Porosity
$\mu+\sigma$	0.47	0.83
μ	0.35	0.50
$\mu-\sigma$	0.22	0.20

After infiltration of pores by cells, the porosity of nano-fibrous web was measured by counting dark and light pixels by using Equation 1.

For each cell, a unique matrix (C) was designed. This matrix contains the fiber area and pores as 0 and 1, and could perform as a mask. By moving this mask through the entire binary image and employing of Equation 2, it is possible to recognize the pores. The diamond cell and the corresponding matrix are shown in Figure 5.

$$A = \sum_{i=1}^{m}\sum_{j=1}^{n} B_{(i+\text{row}(C),\, j+\text{column}(C))} \times C \tag{2}$$

m and n are the number of rows and columns in the binary image and B shows the part of binary image that has the same dimension of matrix C. If all element of the matrix A are equal to zero, it means that B is a pore space in the binary image which can contain the cell C and this section in the binary image corresponding to matrix B is replaced matrix C. By this method, a pore space is not counted more than one time and the number of cells in the binary image with various thresholds can be obtained. As shown in Figure 6, ellipse cells with 2 sizes are infiltrated through the filter media in three different layers.

Infiltration of nano-fibrous filter media with cells of various shapes and dimensions was carried out using the proposed approach.

TABLE II
NUMBER OF INFILTRATED CELLS INTO THE NANO-FIBROUS FILTER MEDIA

Diameter (nm)	120			240			360			480			600		
Threshold	μ+σ	μ	μ-σ	μ+σ	μ	μ-σ	μ+σ	μ	μ-σ	μ+σ	μ	μ-σ	μ+σ	μ	μ-σ
Circle	1640	819	230	327	140	25	121	40	7	58	16	4	33	10	1
Square	2729	1417	401	598	250	54	220	72	13	103	33	6	53	14	1
Ellipse 0	2526	1333	379	635	302	66	247	96	18	131	48	8	71	23	4
Ellipse 25	2694	1409	414	605	280	60	252	96	18	116	37	7	66	22	4
Ellipse 45	2855	1515	430	613	280	54	247	97	18	118	37	6	66	19	4
Ellipse 70	2630	1347	374	602	264	49	230	87	16	112	39	7	65	15	4
Ellipse 90	2480	1284	356	627	284	54	231	87	13	117	34	6	67	18	4
Diamond	2103	1055	264	495	211	34	185	63	10	89	26	4	47	12	1

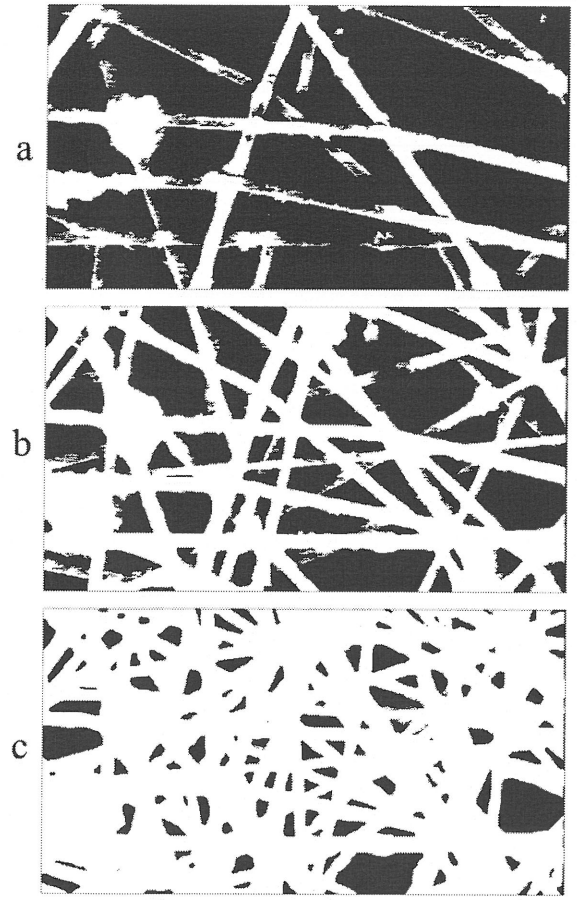

Fig. 3. Binary images of nano-fibrous filter media in various thresholds, a) μ+σ, b) μ, c) μ-σ

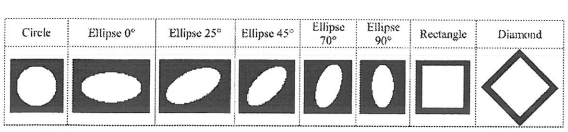

Fig. 4. Various cells' shapes.

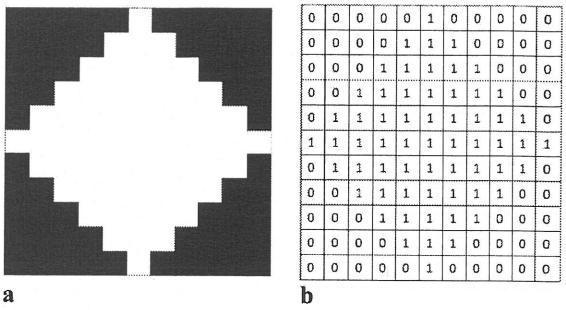

Fig. 5. a diamond cell, b) the binary matrix for diamond cell

The numbers of cells that were infiltrated through the fibrous media are presented in Tables II. The diameters of presented cells were 120, 240, 360, 480, 600 nm (the major diameter is reported for the ellipse cells and the minor diameter is half of the major diameter).

By increasing the threshold value and increasing the depth of layer, the pore surface area decreased. As a result, the lower number of cells could be infiltrated into the layers inside the filter media (Table II). This result shows that the cake was forming mainly on the surface of filter media, and this was confirmed by [17]. Table II shows that the number of infiltrated cells is lower for larger cells than smaller cells. Since in this simulation each cell represented a particle, it can be inferred from this result that the cake was forming faster when the air stream was carrying the larger particles. Maze's study confirms this result [9]. In his simulation the cake formation was faster when the nano-fibrous filter media removed the larger particles similar.

Pressure drop for a clogged filter media (ΔP) was considered as the sum of the pressure drop in the clean filter media (ΔP_0) and the pressure drop resulting from the cake (ΔP_1), according to Eq. (3). As Eq. (4) shows the pressure drop across the cake (ΔP_1) is a function of the cake porosity (ε).

TABLE III
CAKE POROSITY FOR CELLS OF VARIOUS SHAPES AND SIZES, A) 120 NM, B) 240 NM, C) 360 NM, D) 480 NM, E) 600 NM.

Diameter (nm)	120			240			360			480			600		
Threshold	μ+σ	μ	μ-σ	μ+σ	μ	μ-σ	μ+σ	μ	μ-σ	μ+σ	μ	μ-σ	μ+σ	μ	μ-σ
Circle	0.20	0.17	0.08	0.31	0.25	0.12	0.38	0.32	0.13	0.44	0.36	0.13	0.47	0.36	0.15
Square	0.17	0.14	0.07	0.24	0.23	0.11	0.33	0.30	0.13	0.40	0.33	0.13	0.47	0.37	0.15
Ellipse 0	0.22	0.16	0.07	0.29	0.22	0.11	0.34	0.28	0.12	0.38	0.31	0.13	0.44	0.34	0.14
Ellipse 25	0.21	0.16	0.07	0.30	0.23	0.11	0.34	0.29	0.13	0.42	0.34	0.13	0.46	0.35	0.14
Ellipse 45	0.20	0.15	0.07	0.30	0.24	0.11	0.36	0.29	0.13	0.41	0.34	0.14	0.46	0.36	0.14
Ellipse 70	0.22	0.17	0.08	0.29	0.24	0.12	0.37	0.30	0.13	0.43	0.33	0.13	0.46	0.38	0.14
Ellipse 90	0.23	0.17	0.08	0.29	0.23	0.12	0.37	0.30	0.13	0.42	0.35	0.14	0.45	0.36	0.14
Diamond	0.19	0.16	0.08	0.27	0.24	0.12	0.36	0.31	0.13	0.43	0.35	0.14	0.49	0.38	0.15

TABLE IV
NUMBER OF CELLS THAT COULD BE INFILTRATED THROUGH FIBROUS FILTER MEDIA

Threshold	μ+σ					μ					μ-σ				
Diameter (nm)	120	240	360	480	600	120	240	360	480	600	120	240	360	480	600
Circle	296	48	19	9	33	231	43	9	6	10	126	7	2	2	1
Aquare	416	91	34	21	53	373	83	18	13	14	195	20	4	4	1
Ellipse 0	361	96	27	15	71	326	71	22	12	23	153	26	7	1	4
Ellipse 25	438	86	36	17	66	370	67	28	8	22	188	25	4	1	4
Ellipse 45	462	84	38	18	66	389	70	25	14	19	210	20	4	1	4
Ellipse 70	403	95	31	21	65	360	66	22	20	15	190	16	4	1	4
Ellipse 90	367	90	36	18	67	325	81	30	9	18	165	22	4	1	4
Diamond	357	85	21	20	47	333	66	16	7	12	153	7	3	3	1

$$\Delta P = \Delta P_0 + \Delta P_1 \tag{3}$$

$$\Delta P_1 = U_0 m \frac{h_k a_g^2 (1-\varepsilon)\mu}{[C_c \varepsilon^3 \rho_p]} \tag{4}$$

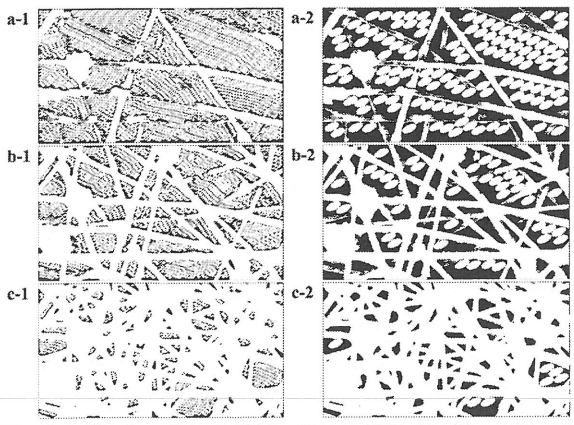

Fig. 6. Infiltration of nano-fibrous filter media with ellipse 25° cells of threshold, a) μ+σ , b) μ, c) μ-σ with diameter of (1) 120 nm and (2) 480 nm.

Where, U_0 is the velocity (m/s), m is the mass of collected particles per unit filter area (g/m^2), h_k is the Kozeny constant, a_g is the particle specific area (m^{-1}), C_c is the Cunningham slip correction factor, and ρ_p is the particle density [17].

After infiltration of nano-fibrous filter media using the proposed approach, the cake porosity for infiltrated media was determined (Table III). Increase in the size of simulated particles caused the cake porosity to increase, and as a result the cake pressure drop also decreased. Thomas' study indicates that the larger particles cause the lower pressure drop [17]. Al-Otoom explained the increases of the pressure drop in filtration of smaller particles as a result of lower porosity of the cake, which is constituted of the smaller particles [12].

In this research the particles and nano-fibrous are considered as solid materials which means that no deformation could be possible for them however, in practical application they are slightly flexible. By considering solid assumption, X numbers of particles can be filtered and the porosity percentage would be Pro%, however during the filtration process, the structure of the filter and the shape of the particles change due to passing

air pressure through the filter. So the particles would be compacted to each other and X+ΔX particles are included into the filter. Consequently, the porosity percentage would be Pro%-ΔPro%. It must be noted as the deformation of inner structure of nano-fibrous far from the particles, thus the value of ΔPro% is negligible (ΔX and ΔPro% are the increase in the numbers of infiltrated particles and decrease in the porosity percentage, respectively).

TABLE V
CAKE POROSITIES FOR THE SAME CELLS OF VARIOUS SIZES

threshold	μ+σ	μ	μ-σ
circle	0.20	0.16	0.08
square	0.16	0.14	0.07
ellipse 0	0.20	0.15	0.07
ellipse 25	0.20	0.15	0.07
ellipse 45	0.19	0.15	0.07
ellipse 70	0.20	0.16	0.08
ellipse 90	0.20	0.16	0.08
diamond	0.19	0.16	0.08

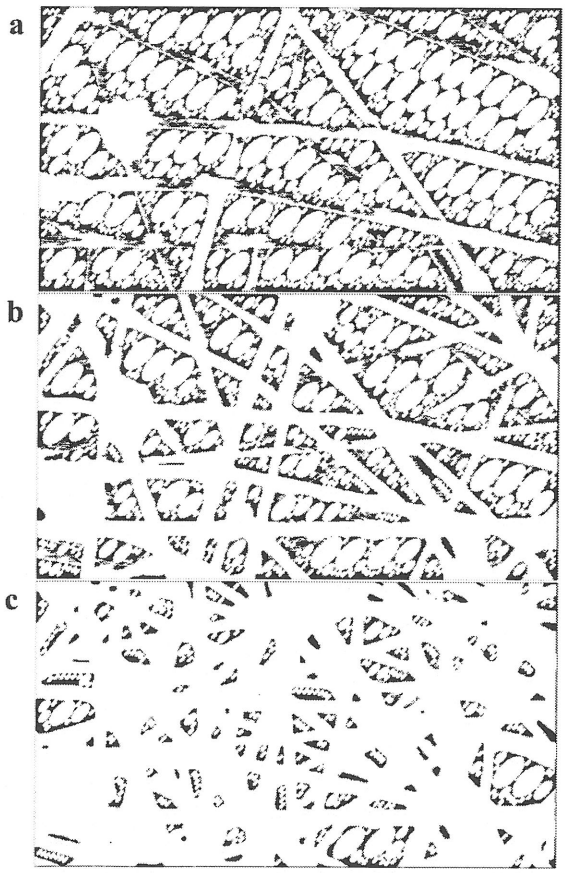

Figure 7 - Infiltration of nano-fibrous filter media with ellipse-45 cell with various diameters, a) threshold: μ+σ, b) threshold: μ, c) threshold: μ-σ.

V. CAKE FORMATION OF PARTICLES OF DIFFERENT SIZES

The presented results in Tables II and III are based on the assumption that the air stream carried the particles of the same size. Since in real condition particles of various sizes are present in the air stream, the image processing algorithm was revised to consider the particles of various sizes in infiltration of filter media and determination of the cake porosity. In the new approach, for each shape, the largest to smallest cells were respectively infiltrated into the binary images resulting from three different thresholds as shown in Figure 7 and the numbers of infiltrated cells are shown in Table IV. By counting the white and dark pixels, cake porosity was determined using Eq. (1) and the results are shown in Table V. The results indicated that the cake porosity was less when the air stream contains particles of various sizes.

VI. CONCLUSION

The simulation of cake formation in the filtration process for particles of various shapes, sizes and configurations was conducted using a new image analysis method. The results showed that the increases of particle size led to increase of cake porosity. Cake formation was faster when the air stream containing larger particles. The presented results were in good agreement with the previous researches. The simulation was revised in order to consider cake formation over the filter media for particles of the same shape but different diameters. The results showed that cake porosity decreased when particles with various sizes were carried by the air stream.

REFERENCES

[1] Q. Zhang, J. Welch, H. Park, C. Wu, W. Sigmund and J. C. M. Marijnissen, "Improvement in nanofiber filtration by multiple thin layers of nanofiber mats", *J. Aerosol Sci.*, vol. 41, no. 2, pp. 230–236, 2010.

[2] K. Yoon, K. Kim, X. Wang, D. Fang, B. S. Hsiao and B. Chu, "High flux ultrafiltration membranes based on electrospun nano-fibrous PAN scaffolds and chitosan coating", *Polymer*, vo. 47, no. 7, pp. 2434–2441, 2006.

[3] R. S. Barhate and S. Ramakrishna, "Nanofibrous filtering media: Filtration problems and solutions from tiny materials", *J. Membrane Sci.*, vol. 296, no. 1-2, pp. 1–8, 2007.

[4] A. C. B. Neiva and J. Leonardo Goldstein, "A procedure for calculating pressure drop during the build-up of dust filter cakes", *Chem. Eng. Process.*, vol. 42, no. 6, pp. 495–501, 2003.

[5] M. Saleem, R. Ullah Khan, M. Suleman Tahir and G. Krammer, "Experimental study of cake formation on heat treated and membrane coated needle felts in a pilot scale pulse jet bag filter using optical in-situ cake height measurement", *Powder Technol.*, vol. 214, no. 3, pp. 388-399, 2011.

[6] M. Saleem, and G. Krammera, "Effect of filtration velocity and dust concentration on cake formation and filter operation in a pilot scale jet pulsed bag filter", *J. Hazard. Mater.*, vol. 144, no. 3, pp. 677–681, 2007.

[7] R. Bai and C. Tien, "Further work on cake filtration analysis, *Chem. Eng. Sci.*, vol. 60, no. 2, pp. 301–313, 2005.

[8] C. B. Song, H. S. Park and K. W. Lee, "Experimental study of filter clogging with monodisperse PSL particles", *Powder Technol.*, vol. 163, no. 3, pp. 152–159, 2006.

[9] B. Maze, H. Vahedi Tafreshi, Q. Wang and B. Pourdeyhimi, "A simulation of unsteady-state filtration via nanofiber media at reduced operating pressures", *J. Aerosol Sci.*, vol. 38, no. 5, pp. 550–571, 2007.

[10] C. L. Lin and J. D. Miller, "Pore structure and network analysis of filter cake", *Chem. Eng. J.*, vol. 80, no. 1-3, pp. 221–231, 2000.

[11] A. Joubert, J. C. Laborde, L. Bouilloux, S. Chazelet and D. Thomas, "Modelling the pressure drop across HEPA filters during cake filtration in the presence of humidity", *Chem. Eng. J.*, vol. 166, no. 2, pp. 616–623, 2011.

[12] A. Y. Al-Otoom, "Prediction of the collection efficiency, the porosity, and the pressure drop across filter cakes in particulate air filtration", *Atmos. Environ.*, vol. 39, no. 1, pp. 51–57, 2005.
[13] M. Ziabari, V. Mottaghitalab, S. T. McGovern and A. K. Haghi, "A new image analysis based method for measuring electrospun nanofiber diameter", *Nanoscale Res Lett*, vol. 2, no. 12, pp. 597–600, 2007.
[14] L. Ghasemi-Mobarakeh, D. Semnani and M. Morshed, "A novel method for porosity measurement of various surface layers of nanofibers mat using image analysis for tissue engineering applications", *J. Appl. Polym. Sci.*, vol. 106, no. 4, pp. 2536–2542, 2007.
[15] D. Semnani, L. Ghasemi-Mobarakeh, M. Morshed and M. Nasr-Esfahani, "A novel method for the determination of cell infiltration into nanofiber scaffolds using image analysis for tissue engineering applications", *J. Appl. Polym. Sci.*, vol. 111, no. 1, pp. 317–322, 2009.
[16] L. Boskovic, I. E. Agranovski, I. S. Altman and R. D. Braddock, "Filter efficiency as a function of nanoparticle velocity and shape", *Aerosol Sci.*, vol. 39, no. 7, pp. 635–644, 2008.
[17] D. Thomas, P. Penicot, P. Contal, D. Leclerc and J. Vendel, "Clogging of fibrous filters by solid aerosol particles Experimental and modelling study", J. *Chem. Eng. Sci.*, vol. 56, no. 11, pp. 3549–3561, 2001.